

The JAK/STAT3 and NF- κ B signaling pathways regulate cancer stem cell properties in anaplastic thyroid cancer cells.

Ken Shiraiwa^{1,4}, Michiko Matsuse¹, Yuka Nakazawa², Tomoo Ogi², Keiji Suzuki¹, Vladimir Saenko³, Shuhang Xu¹, Kazuo Umezawa⁵, Shunichi Yamashita¹, Kazuhiro Tsukamoto⁴, Norisato Mitsutake¹

¹Departments of Radiation Medical Sciences, ²Genome Repair, ³Radiation Molecular Epidemiology, Atomic Bomb Disease Institute, Nagasaki University. ⁴Department of Pharmacotherapeutics, Nagasaki University Graduate School of Biomedical Sciences.

⁵Department of Molecular Target Medicine, Aichi Medical University School of Medicine

Ken Shiraiwa, MS

Department of Radiation Medical Sciences, Atomic Bomb Disease Institute, Nagasaki University. 1-12-4 Sakamoto, Nagasaki 852-8523, Japan.

Department of Pharmacotherapeutics, Nagasaki University Graduate School of Biomedical Sciences. 1-7-1 Sakamoto, Nagasaki 852-8501, Japan

eine.kleine.nachtmusik.k525@gmail.com

Michiko Matsuse, PhD

Department of Radiation Medical Sciences, Atomic Bomb Disease Institute, Nagasaki University. 1-12-4 Sakamoto, Nagasaki 852-8523, Japan.

michikom@nagasaki-u.ac.jp

Yuka Nakazawa, PhD

Department of Genome Repair, Atomic Bomb Disease Institute, Nagasaki University. 1-12-4 Sakamoto, Nagasaki 852-8523, Japan.

Current address: Department of Genetics, Research Institute of Environmental Medicine, Nagoya University. Furo-cho, Chikusa-ku, Nagoya 464-8601, Japan

yu-naka@riem.nagoya-u.ac.jp

Tomoo Ogi, PhD

Department of Genome Repair, Atomic Bomb Disease Institute, Nagasaki University. 1-12-4 Sakamoto, Nagasaki 852-8523, Japan.

togi@nagasaki-u.ac.jp

Current address: Department of Genetics, Research Institute of Environmental Medicine, Nagoya University. Furo-cho, Chikusa-ku, Nagoya 464-8601, Japan

togi@riem.nagoya-u.ac.jp

Keiji Suzuki, PhD

Department of Radiation Medical Sciences, Atomic Bomb Disease Institute, Nagasaki University. 1-12-4 Sakamoto, Nagasaki 852-8523, Japan.

kzsuzuki@nagasaki-u.ac.jp

Vladimir Saenko, PhD

Department of Radiation Molecular Epidemiology, Atomic Bomb Disease Institute, Nagasaki University. 1-12-4 Sakamoto, Nagasaki 852-8523, Japan.

saenko@nagasaki-u.ac.jp

Shuhang Xu, MD PhD

Department of Radiation Medical Sciences, Atomic Bomb Disease Institute, Nagasaki University. 1-12-4 Sakamoto, Nagasaki 852-8523, Japan.

shuhangxu@vip.163.com

Kazuo Umezawa, PhD

Department of Molecular Target Medicine, Aichi Medical University School of Medicine. Nagakute, Aichi 480-1195, Japan.

omezawa@aichi-med-u.ac.jp

Shunichi Yamashita, MD PhD

Department of Radiation Medical Sciences, Atomic Bomb Disease Institute, Nagasaki University. 1-12-4 Sakamoto, Nagasaki 852-8523, Japan.

shun@nagasaki-u.ac.jp

Kazuhiro Tsukamoto, MD PhD

Department of Pharmacotherapeutics, Nagasaki University Graduate School of Biomedical Sciences. 1-7-1 Sakamoto, Nagasaki 852-8501, Japan

ktsuka@nagasaki-u.ac.jp

Norisato Mitsutake, MD PhD

Department of Radiation Medical Sciences, Atomic Bomb Disease Institute, Nagasaki University. 1-12-4 Sakamoto, Nagasaki 852-8523, Japan.

mitsu@nagasaki-u.ac.jp

Running title: JAK3/STAT3/NF- κ B regulates CSC properties in ATC cells

Keywords: JAK, STAT3, NF- κ B, cancer stem cells, anaplastic thyroid carcinoma

Correspondence to:

Norisato Mitsutake, MD PhD

Department of Radiation Medical Sciences

Atomic Bomb Disease Institute

Nagasaki University

1-12-4 Sakamoto, Nagasaki 852-8523, Japan

Tel: +81-95-819-7116

Fax: +81-95-819-7117

mitsu@nagasaki-u.ac.jp

Abstract

Background: Anaplastic thyroid carcinoma (ATC) is one of the most aggressive and refractory cancers, and a therapy with a new concept needs to be developed. Recently, the research of cancer stem cells (CSCs) has been progressed, and CSCs have been suggested to be responsible for metastasis, recurrence, and therapy resistance. In ATC-CSCs, aldehyde dehydrogenase (ALDH) activity is the most reliable marker to enrich the CSCs; however, it itself is just a marker and is not involved in CSC properties. In the present study, therefore, we aimed to identify key signaling pathways specific for ATC-CSCs.

Methods: A siRNA library targeting 719 kinases was used in a sphere formation assay and cell survival assay using ATC cell lines to select target molecules specific for CSC properties. The functions of the selected candidates were confirmed by sphere formation, cell survival, soft-agar, and nude mice xenograft assays using small compound inhibitors.

Results: We focused on *PDGFR*, *JAK*, and *PIM*, whose siRNAs had a higher inhibitory effect on sphere formation and also a lower or no effect on regular cell growth in both FRO and KTC3 cells. Next, we used inhibitors of *PDGFR*, *JAK*, *STAT3*, *PIM* and *NF-κB*, and all of them successfully suppressed sphere formation in a dose-dependent manner but not regular cell growth, conforming the screening results. Inhibition of the *JAK/STAT3* and *NF-κB* pathways also reduced anchorage-independent growth in soft agar and tumor growth in nude mice.

Conclusions: These results suggest that *JAK/STAT3* and *NF-κB* signals play important roles in ATC-CSCs. Targeting these signaling pathways may be a promising approach to treat ATC.

Introduction

Thyroid carcinoma is the most common endocrine malignancy and its incidence is growing worldwide. More than 90% of thyroid carcinomas are differentiated types consisting of papillary thyroid carcinoma (PTC) and follicular thyroid carcinoma (FTC), and their overall prognosis is favorable. However, anaplastic thyroid carcinoma (ATC), which is an undifferentiated type accounting for 1–2% of all thyroid cancer cases, is one of the deadliest human neoplasms, and its mean survival is less than one year even with multimodal treatments (1, 2). To overcome this situation, a therapy with a new concept needs to be developed.

In recent years, the cancer stem cell (CSC) theory has emerged as an attractive model to explain many aspects of carcinogenesis including metastasis, recurrence, and therapy resistance (3, 4). CSCs are a small subpopulation in the cancer tissue and either self-renew or give rise to non-CSCs to produce heterogeneous tumors. Conventional chemo- and radio-therapy have been developed to target non-CSCs, but CSCs are highly resistant to these treatments. Thus, targeting CSCs is a reasonable approach to treat refractory cancers such as ATC.

In ATC, previous studies have identified several biomarkers to enrich CSCs. Among these markers, aldehyde dehydrogenase (ALDH) activity is the most reliable and widely used (5, 6). Todaro *et al.* have identified CSCs as a small subpopulation with high ALDH activity; the CSCs were highly tumorigenic in immunocompromised mice while non-CSCs were not (5). However, the ALDH activity itself is just a marker and does not have a functional role in CSC properties (7). To target CSCs, it is necessary to identify functional molecules that are important for survival and self-renewal of CSCs, rather than a marker. In the present study, we focused on kinases as targets because they are an important component of cell signaling pathways and can be blocked by small compounds. If inhibiting different molecules on a same signaling pathway is effective to suppress CSC properties, it is convincing that the pathway is important, which increases the possibility of developing clinical applications.

In this study, we used a siRNA library targeting 719 kinases to screen for important molecules for CSC properties. As a result, the JAK–STAT3–NF- κ B signaling cascade emerged. Several inhibitors of this pathway successfully suppressed some CSCs abilities but not growth of regular cancer cells, suggesting that this pathway is important for CSC functions and may be an attractive target to treat ATC.

Materials and methods

Cell cultures

FRO, KTC3, and THJ16T were established from human ATCs. FRO was obtained from Dr. James Fagin (currently Memorial Sloan-Kettering Cancer Center, NY, USA). KTC3 was kindly provided by Dr. Junichi Kurebayashi (Kawasaki Medical School, Okayama, Japan)(8). THJ16T was obtained from Dr. John Copland (Mayo Clinic, FL, USA). ACT1 was obtained from Dr. Naoyoshi Onoda (Osaka City University; originally established by Dr. Seiji Ohata of Tokushima University (9)). 8505C was provided by the RIKEN BRC through the National Bio-Resource Project of the MEXT, Japan. All cells were cultured in a growth medium (GM) consisting of RPMI1640, 10% fetal bovine serum, and penicillin/streptomycin at 37°C in a humidified atmosphere with 5% CO₂. Cell growth was measured using a Cell Counting Kit-8 (Dojindo). The following inhibitors were used: Imatinib (Novartis), JAK Inhibitor I (Calbiochem), STA-21 (Santa Cruz), AZD1208 (Selleckchem), and DHMEQ (synthesized by KU).

Sphere formation assay

The cells were incubated in serum-free DMED/F-12 (1:1) supplemented with 20 ng/ml EGF, 20 ng/ml bFGF and B27 without vitamin A (Thermo Fisher Scientific) in a HydroCell plate (CellSeed). Spheres with a diameter of 100 μ m or more were counted. Images were captured using a phase contrast microscope (Olympus). Combination drug effects on sphere formation were evaluated using CompuSyn software (ComboSyn).

siRNA screening

A MISSION siRNA Human Kinase Panel (Sigma-Aldrich) was used. This panel includes siRNAs for 719 human kinase genes. For sphere formation, cells were seeded in a 96-well HydroCell plate, and each siRNA was transfected at 10 nM using X-treme GENE siRNA transfection reagent (Roche). For each gene, three different siRNAs were mixed and used in the same well. After incubating for 96 hours, the cells were stained with Hoechst 33342 (Sigma-Aldrich), and $\geq 100 \mu\text{m}$ spheres were counted using an ArrayScan VTI (Thermo Fisher Scientific). For regular cell growth, cells were seeded in a regular 96-well plate, and transfection was performed as described above. After incubation for 96 hours, cell viability was determined using a Cell Counting Kit-8. For control, cells were transfected with Cy3-labeled scrambled RNA. Transfection efficiency was determined by a fluorescent microscope, and it was almost 100%.

Soft agar colony formation assay

Cells were mixed with 0.33% agar/GM and plated on a solidified 0.5% agar/GM. The agar layers were further overlaid with the GM containing appropriate concentrations of the inhibitors that were replaced every 2–3 days. After incubation for 10 (FRO cells) or 20 (THJ16T cells) days, images were captured using a digital camera, and the number of colonies was counted using Fiji software (10).

In vivo xenograft experiments

All procedures were conducted in accordance with the principles and procedures outlined in the Guide for the Care and Use of Laboratory Animals of Nagasaki University with approval of the institutional animal care and use committee. FRO cells (1×10^6) resuspended in the growth medium were injected s.c. into both flanks of 6-week-old male BALB/c *nu/nu* mice (CLEA Japan). Then they were randomly assigned into three groups. Tumor volumes were calculated according to the formula: $a^2 \times b \times 0.4$, where a is the smallest tumor diameter and b is the diameter perpendicular to a . STA-21 or DHMEQ solution in DMSO/PBS (ratio 1:1) was injected *i.p.* daily for one week, beginning from day 1 after tumor cell implantation. Control group mice received vehicle injections only.

ALDEFLUOR assay

To measure the ALDH activity, cells were labeled using an ALDEFLUOR assay kit (StemCell Technologies) following the manufacturer's protocol. The cells were then analyzed using a FACSJazz cell sorter (BD Biosciences). The data were further processed with FlowJo software (FlowJo).

Statistical Analysis

Differences between groups were examined for statistical significance with one-way ANOVA followed by Tukey's post test. A *p*-value not exceeding 0.05 was considered statistically significant. Data were analyzed with PRISM 6 software (GraphPad Software).

Results

siRNA screening to identify important cell signaling for CSC properties.

We and others have demonstrated that sphere formation assay is valuable to evaluate CSC properties (3, 4, 6). In our previous report using eight thyroid cancer cell lines, the ability of sphere formation perfectly corresponded to that of tumor formation in mice, which is important evidence for the presence of CSCs (6). It is also applicable to high-throughput screening. In the present study, we combined the use of a siRNA library for 719 kinase genes with the sphere formation assay. First, FRO cells were transfected with all siRNAs included in the library, and the sphere formation assay was performed. We also measured cell survival in the regular growth condition after the transfection. To identify specific cell signaling for CSC properties, sphere/survival ratios were calculated. When the ratio is small, it suggests that only sphere formation but not regular cell growth is blocked. The top 100 genes were selected and were further subjected to the second screening using another ATC cell line, KTC3. In the second screening, the sphere/survival ratios were equally analyzed. The siRNA target genes with the lowest ratios are listed in Table 1 (1st screening in FRO cells) and Table 2 (2nd screening in KTC3 cells). Among these genes, we focused on *PDGFR*, *JAK*, and *PIM* because they are members of the cell signaling cascade depicted in Fig. 1.

Specific inhibitors suppressed sphere formation but not cell survival.

To confirm the significance of the above signaling pathway, we treated the cells with various inhibitors and examined the sphere formation ability and regular cell survival. The following inhibitors were used: imatinib, a PDGFR inhibitor; JAK inhibitor I, a pan-JAK inhibitor; STA-21, a STAT3 inhibitor; AZD1208, a pan-PIM inhibitor; and DHMEQ, a NF- κ B inhibitor (Fig. 1). In FRO cells, all of the inhibitors suppressed sphere formation in a dose-dependent manner (Fig. 2A, left). At higher concentrations, the differences were statistically significant. On the other hand, regular cell growth was not affected at the same concentrations used in the sphere formation assay (Fig. 2A, right). We also used KTC3 cells and obtained similar data (Fig. 2B). Representative sphere images are shown in Supplementary Figure S1a and b. These data suggest that the signaling cascade, PDGFR–JAK–STAT3–PIM–NF- κ B, has a significant role in CSC properties but not in regular cell growth.

Since the JAK/STAT3 and NF- κ B pathways are basically two different signaling pathways, we tested the effect of the combination of two inhibitors, STA-21 and DHMEQ. Based on the results presented in Fig. 3A, the combination index (CI) was calculated. The combination effects were synergistic in FRO cells (CI range: 0.53–0.89) and almost additive in KTC3 cells (CI range: 1.00–1.11).

We also checked whether these inhibitors suppress sphere formation in other ATC cell lines. Although effect sizes were different, both inhibitors significantly reduced the number of spheres in 8505C and ACT1 cells (Fig. 3B).

Colony formation in soft agar

Next, to investigate the significance of the signaling pathway on the ability of anchorage-independent growth, which is also an important characteristic of tumorigenicity of cells, we performed colony formation assays in soft agar. We used two inhibitors, JAK inhibitor I and DHMEQ to block JAK and NF- κ B, respectively. In FRO cells, both JAK inhibitor I and DHMEQ reduced the number of colonies in a dose-dependent manner (Fig. 4A, left). At higher concentrations, the differences were statistically significant.

Unfortunately, colony formation in KTC3 cells was defective even in the absence of the inhibitors. We therefore used THJ16T cells, another tumorigenic ATC cell line, in which sphere formation was also suppressed with the inhibitors (Fig. 4A, right). Similarly, the colony formation after treatment with JAK inhibitor I or DHMEQ was suppressed (Fig. 4A, middle). Within the range of concentrations we used, the suppressive effect of JAK inhibitor I was stronger than that of DHMEQ in both cell lines (Fig. 4).

Tumor formation in nude mice

To examine the effect of inhibitors for the STAT3 and NF- κ B pathways on *in vivo* tumor growth, we performed xenograft experiments using nude mice. To see the effect on tumor initiation, we started the treatment from day 1 after cell implantation. Starting from day 21, tumor size in mice treated with STA-21 or DHMEQ was significantly smaller than that in control mice (Fig. 4B).

Suppression of the JAK pathway did not alter ALDH activity.

Our and others' previous studies have demonstrated that ALDH activity is the most reliable marker for CSCs in ATC cells (5, 6). The ALDEFLUOR assay is a standard procedure to measure ALDH activity in each living cell. We treated FRO and THJ16T cells with JAK inhibitor I for one week and then performed the ALDEFLUOR assay to investigate the impact of inhibiting the pathway on the activity. Diethylaminobenzaldehyde (DEAB), a specific inhibitor of ALDH, was used to measure background fluorescence. As shown in Fig. 5, the treatment with JAK inhibitor I did not reduce the proportion of the ALDH-positive population in both FRO and THJ16T cells. These results suggest that ALDH function is not directly associated with CSC properties.

Discussion

In the present study, we have successfully identified that the PDGFR–JAK–STAT3–PIM–NF- κ B signaling cascade plays an important role in CSC functions in ATC. There are a number of studies reporting that STAT3 signaling is important for CSCs in a variety of cancer types such as breast cancer (11-14), hepatocellular carcinoma (15, 16), prostate cancer (17, 18), lung cancer (19), ovarian cancer (20), and glioblastoma (21). However, in

ATC, there is only one report showing that STAT3 plays a key role in mediating CSC properties in ATC cells (22). In this study, CSCs were enriched in the CD133-positive population, and Cucurbitacin I, a STAT3 inhibitor, suppressed the sphere-forming ability and increased sensitivities to radio-chemotherapy. However, these effects were also observed in the CD133-negative cells. One possible explanation is that CD133 may not be a precise marker to select CSCs in ATC. Unfortunately, the positive rates of CD133 were not shown in this study. In our previous work, we did not find any CD133-positive cells in the five ATC cell lines, FRO, KTC2, KTC3, ACT1, and 8505C, and concluded that CD133 is not a suitable marker for CSCs in ATC (6). We cannot explain this discrepancy. Since little is known about the specific cell signaling/marker in ATC-CSCs, further studies are definitely needed in this field.

Couto *et al.* have reported that STAT3 is a negative regulator of tumor growth in PTC (23). Although they did not focus on CSCs, tumorigenesis in mice was enhanced after STAT3 inhibition, implying that STAT3 is a tumor suppressor also in PTC-CSCs. STAT3 function may be different between ATC and PTC. These findings suggest that it remains to be studied whether targeting STAT3 is effective to block anaplastic transformation from PTC to ATC.

It has been demonstrated that STAT3 inhibition reduces resistance to chemotherapy in ATC cells (24). However, this study also did not separate and use the CSC fraction. In the present study, regular cell growth was not affected, but sphere formation and anchorage-independent growth were suppressed by the JAK/STAT3 inhibitors at the used concentrations. Generally, the ability of sphere formation and anchorage-independent growth reflects CSC properties, and therefore, we conclude that STAT3 signaling is important for CSC properties in ATC.

NF- κ B signaling plays an important role in CSCs of various types of malignancies including leukemia, glioblastoma, prostate cancer, ovarian cancer, breast cancer, pancreatic cancer, and colon cancer (25). However, as far as we know, this study is the first to show its importance in ATC-CSCs. Indeed, NF- κ B signaling is activated not only in CSCs but also in all ATC cells (26, 27); however, our present study indicates that NF- κ B is crucial

especially in CSCs. According to our results, there is a possibility that the treatment with low concentration of NF- κ B inhibitors is effective to suppress CSC functions. Since chemoresistance of CSCs is usually high, a combination of the NF- κ B inhibition and chemotherapeutics may be an attractive strategy.

There are multiple crosstalks between the JAK/STAT3 and NF- κ B signaling pathways. As mentioned, the STAT3 signal is transduced to NF- κ B via PIM (28, 29). In addition, the activated NF- κ B signal leads to production and secretion of IL-6, and then IL-6 activates the STAT3 signaling pathway in an autocrine/paracrine fashion (30, 31). Moreover, STAT3 interacts with RelA, a p65 subunit of NF- κ B, and recruits p300. Then, p300 acetylates RelA, leading to nuclear retention of RelA and thereby sustaining its transcriptional activity (32). There is a possibility that these crosstalks influence each other also in ATC-CSCs. In the present study, the treatment with AZD1208 alone suppressed sphere formation substantially. However, this does not necessarily mean that the STAT3–PIM–NF- κ B cascade is the most important for CSC properties in ATC because PIM also has other functions such as activating MYC and inhibiting ROS (28). Our experiments demonstrate that the effect of the combination of STAT3 and NF- κ B inhibitors was synergistic in FRO cells and almost additive in KTC3 cells, suggesting that the degree of the interaction between the two pathways, JAK/STAT3 and NF- κ B, depends on the cell type.

In nude mice xenograft experiments, we started the treatment one day after tumor cell implantation to see the effect of the drugs on tumor initiation. Tumors treated with STA-21 or DHMEQ were statistically smaller than those in control mice after day 21, suggesting that these drugs successfully reduced the number of CSCs. Note that non-CSCs have plasticity allowing to generate CSCs in thyroid cancer cell lines (6, 33), which may, in part, be involved in tumor formation in mice treated with the drugs. Nevertheless, these results support the potential clinical benefit of targeting the JAK/STAT3 and NF- κ B pathways in ATCs.

As previously reported, the ALDH function itself is not involved in CSC properties in ATC (7). Our results indicate that ALDH activity is not regulated by the JAK/STAT3 signaling pathway, consistent with the above study. There may be a common upstream

molecule but further studies are still necessary to clarify the regulation of the ALDH activity in ATC-CSCs.

In conclusion, the present study demonstrates that the JAK/STAT3 and NF- κ B signaling pathways play important roles in ATC-CSCs. Interference with these pathways may provide a novel approach for ATC treatment.

Acknowledgements

This work was supported in part by JSPS KAKENHI Grant Numbers 25861110 (MM), 26293222 (SY). We thank Dr. James Fagin (Memorial Sloan-Kettering Cancer Center), Dr. Junichi Kurebayashi (Kawasaki Medical School), Dr. John Copland (Mayo Clinic), and Dr. Naoyoshi Onoda (Osaka City University) for providing the FRO, KTC3, THJ16T, and ACT1 cells, respectively.

Disclosure Statement

The authors have nothing to disclose.

References

1. Spielman DB, Badhey A, Kadakia S, Inman JC, Ducic Y 2017 Rare Thyroid Malignancies: an Overview for the Oncologist. *Clin Oncol (R Coll Radiol)* **29**:298-306.
2. Sipos JA, Mazzaferri EL 2010 Thyroid cancer epidemiology and prognostic variables. *Clin Oncol (R Coll Radiol)* **22**:395-404.
3. Maenhaut C, Dumont JE, Roger PP, van Staveren WC 2010 Cancer stem cells: a reality, a myth, a fuzzy concept or a misnomer? An analysis. *Carcinogenesis* **31**:149-158.
4. Nagayama Y, Shimamura M, Mitsutake N 2016 Cancer Stem Cells in the Thyroid. *Front Endocrinol (Lausanne)* **7**:20.
5. Todaro M, Iovino F, Eterno V, Cammareri P, Gambarà G, Espina V, Gulotta G, Dieli F, Giordano S, De Maria R, Stassi G 2010 Tumorigenic and metastatic activity of human thyroid cancer stem cells. *Cancer Res* **70**:8874-8885.
6. Shimamura M, Nagayama Y, Matsuse M, Yamashita S, Mitsutake N 2014 Analysis of multiple markers for cancer stem-like cells in human thyroid carcinoma cell lines. *Endocr J* **61**:481-490.
7. Shimamura M, Kurashige T, Mitsutake N, Nagayama Y 2017 Aldehyde dehydrogenase activity plays no functional role in stem cell-like properties in anaplastic thyroid cancer cell lines. *Endocrine* **55**:934-943.
8. Kurebayashi J, Okubo S, Yamamoto Y, Ikeda M, Tanaka K, Otsuki T, Sonoo H 2006 Additive antitumor effects of gefitinib and imatinib on anaplastic thyroid cancer cells. *Cancer Chemother Pharmacol* **58**:460-470.
9. Chung SH, Onoda N, Ishikawa T, Ogisawa K, Takenaka C, Yano Y, Hato F, Hirakawa K 2002 Peroxisome proliferator-activated receptor gamma activation induces cell cycle arrest via the p53-independent pathway in human anaplastic thyroid cancer cells. *Jpn J Cancer Res* **93**:1358-1365.

10. Schindelin J, Arganda-Carreras I, Frise E, Kaynig V, Longair M, Pietzsch T, Preibisch S, Rueden C, Saalfeld S, Schmid B, Tinevez JY, White DJ, Hartenstein V, Eliceiri K, Tomancak P, Cardona A 2012 Fiji: an open-source platform for biological-image analysis. *Nat Methods* **9**:676-682.
11. Zhang H, Cai K, Wang J, Wang X, Cheng K, Shi F, Jiang L, Zhang Y, Dou J 2014 MiR-7, inhibited indirectly by lincRNA HOTAIR, directly inhibits SETDB1 and reverses the EMT of breast cancer stem cells by downregulating the STAT3 pathway. *Stem Cells* **32**:2858-2868.
12. Thakur R, Trivedi R, Rastogi N, Singh M, Mishra DP 2015 Inhibition of STAT3, FAK and Src mediated signaling reduces cancer stem cell load, tumorigenic potential and metastasis in breast cancer. *Sci Rep* **5**:10194.
13. Ibrahim SA, Gadalla R, El-Ghonaimy EA, Samir O, Mohamed HT, Hassan H, Greve B, El-Shinawi M, Mohamed MM, Gotte M 2017 Syndecan-1 is a novel molecular marker for triple negative inflammatory breast cancer and modulates the cancer stem cell phenotype via the IL-6/STAT3, Notch and EGFR signaling pathways. *Mol Cancer* **16**:57.
14. Kim YJ, Kim JY, Lee N, Oh E, Sung D, Cho TM, Seo JH 2017 Disulfiram suppresses cancer stem-like properties and STAT3 signaling in triple-negative breast cancer cells. *Biochem Biophys Res Commun* **486**:1069-1076.
15. Wang X, Sun W, Shen W, Xia M, Chen C, Xiang D, Ning B, Cui X, Li H, Li X, Ding J, Wang H 2016 Long non-coding RNA DILC regulates liver cancer stem cells via IL-6/STAT3 axis. *J Hepatol* **64**:1283-1294.
16. Jiang C, Long J, Liu B, Xu M, Wang W, Xie X, Wang X, Kuang M 2017 miR-500a-3p promotes cancer stem cells properties via STAT3 pathway in human hepatocellular carcinoma. *J Exp Clin Cancer Res* **36**:99.
17. Albino D, Civenni G, Rossi S, Mitra A, Catapano CV, Carbone GM 2016 The ETS factor ESE3/EHF represses IL-6 preventing STAT3 activation and expansion of the prostate cancer stem-like compartment. *Oncotarget* **7**:76756-76768.

18. Wen S, Tian J, Niu Y, Li L, Yeh S, Chang C 2016 ASC-J9((R)), and not Casodex or Enzalutamide, suppresses prostate cancer stem/progenitor cell invasion via altering the EZH2-STAT3 signals. *Cancer Lett* **376**:377-386.
19. Shao C, Sullivan JP, Girard L, Augustyn A, Yenerall P, Rodriguez-Canales J, Liu H, Behrens C, Shay JW, Wistuba, II, Minna JD 2014 Essential role of aldehyde dehydrogenase 1A3 for the maintenance of non-small cell lung cancer stem cells is associated with the STAT3 pathway. *Clin Cancer Res* **20**:4154-4166.
20. Abubaker K, Luwor RB, Zhu H, McNally O, Quinn MA, Burns CJ, Thompson EW, Findlay JK, Ahmed N 2014 Inhibition of the JAK2/STAT3 pathway in ovarian cancer results in the loss of cancer stem cell-like characteristics and a reduced tumor burden. *BMC Cancer* **14**:317.
21. Garner JM, Fan M, Yang CH, Du Z, Sims M, Davidoff AM, Pfeffer LM 2013 Constitutive activation of signal transducer and activator of transcription 3 (STAT3) and nuclear factor kappaB signaling in glioblastoma cancer stem cells regulates the Notch pathway. *J Biol Chem* **288**:26167-26176.
22. Tseng LM, Huang PI, Chen YR, Chen YC, Chou YC, Chen YW, Chang YL, Hsu HS, Lan YT, Chen KH, Chi CW, Chiou SH, Yang DM, Lee CH 2012 Targeting signal transducer and activator of transcription 3 pathway by cucurbitacin I diminishes self-renewing and radiochemoresistant abilities in thyroid cancer-derived CD133+ cells. *J Pharmacol Exp Ther* **341**:410-423.
23. Couto JP, Daly L, Almeida A, Knauf JA, Fagin JA, Sobrinho-Simoes M, Lima J, Maximo V, Soares P, Lyden D, Bromberg JF 2012 STAT3 negatively regulates thyroid tumorigenesis. *Proc Natl Acad Sci U S A* **109**:E2361-2370.
24. Francipane MG, Eterno V, Spina V, Bini M, Scerrino G, Buscemi G, Gulotta G, Todaro M, Dieli F, De Maria R, Stassi G 2009 Suppressor of cytokine signaling 3 sensitizes anaplastic thyroid cancer to standard chemotherapy. *Cancer Res* **69**:6141-6148.
25. Rinkenbaugh AL, Baldwin AS 2016 The NF-kappaB Pathway and Cancer Stem Cells. *Cells* **5**.

26. Starenki DV, Namba H, Saenko VA, Ohtsuru A, Maeda S, Umezawa K, Yamashita S 2004 Induction of thyroid cancer cell apoptosis by a novel nuclear factor kappaB inhibitor, dehydroxymethylepoxyquinomicin. *Clin Cancer Res* **10**:6821-6829.
27. Meng Z, Mitsutake N, Nakashima M, Starenki D, Matsuse M, Takakura S, Namba H, Saenko V, Umezawa K, Ohtsuru A, Yamashita S 2008 Dehydroxymethylepoxyquinomicin, a novel nuclear Factor-kappaB inhibitor, enhances antitumor activity of taxanes in anaplastic thyroid cancer cells. *Endocrinology* **149**:5357-5365.
28. Tursynbay Y, Zhang J, Li Z, Tokay T, Zhumadilov Z, Wu D, Xie Y 2016 Pim-1 kinase as cancer drug target: An update. *Biomed Rep* **4**:140-146.
29. Nihira K, Ando Y, Yamaguchi T, Kagami Y, Miki Y, Yoshida K 2010 Pim-1 controls NF-kappaB signalling by stabilizing RelA/p65. *Cell Death Differ* **17**:689-698.
30. Huang WL, Yeh HH, Lin CC, Lai WW, Chang JY, Chang WT, Su WC 2010 Signal transducer and activator of transcription 3 activation up-regulates interleukin-6 autocrine production: a biochemical and genetic study of established cancer cell lines and clinical isolated human cancer cells. *Mol Cancer* **9**:309.
31. Yu H, Pardoll D, Jove R 2009 STATs in cancer inflammation and immunity: a leading role for STAT3. *Nat Rev Cancer* **9**:798-809.
32. Lee H, Herrmann A, Deng JH, Kujawski M, Niu G, Li Z, Forman S, Jove R, Pardoll DM, Yu H 2009 Persistently activated Stat3 maintains constitutive NF-kappaB activity in tumors. *Cancer Cell* **15**:283-293.
33. Ma R, Minsky N, Morshed SA, Davies TF 2014 Stemness in human thyroid cancers and derived cell lines: the role of asymmetrically dividing cancer stem cells resistant to chemotherapy. *J Clin Endocrinol Metab* **99**:E400-409.

Table 1. 1st screening using the siRNA library for kinases in FRO cells.

Gene	sphere formation (%)	cell survival (%)	sphere/survival ratio	Gene	sphere formation (%)	cell survival (%)	sphere/survival ratio	Gene	sphere formation (%)	cell survival (%)	sphere/survival ratio
<i>PDK4</i>	6.92	130.20	0.05	<i>PRKCD</i>	12.08	87.84	0.14	<i>NME1-NME2</i>	20.54	123.78	0.17
<i>PAK1</i>	7.55	119.59	0.06	<i>EIF2AK4</i>	18.89	134.97	0.14	<i>CSK</i>	22.31	134.35	0.17
<i>IRAK2</i>	12.41	155.40	0.08	<i>LOC442075</i>	19.40	138.02	0.14	<i>PFKFB2</i>	20.21	120.79	0.17
<i>PRKCQ</i>	10.03	112.86	0.09	<i>PRKG1</i>	17.78	124.76	0.14	<i>CHEK1</i>	18.15	108.06	0.17
<i>BMPR1B</i>	10.41	111.26	0.09	<i>PFKM</i>	21.70	150.86	0.14	<i>INSR</i>	24.33	143.77	0.17
<i>PIM3</i>	14.38	135.34	0.11	<i>STK32B</i>	16.40	112.46	0.15	<i>MAP2K1</i>	21.56	126.61	0.17
<i>MAPK7</i>	13.43	120.16	0.11	<i>NPR2</i>	13.31	90.45	0.15	<i>GAK</i>	19.77	115.09	0.17
<i>PLK1</i>	7.47	66.13	0.11	<i>GRK4</i>	15.34	103.79	0.15	<i>MAPKAPK3</i>	23.75	137.27	0.17
<i>GRK6</i>	15.34	135.13	0.11	<i>PRKAB1</i>	18.20	119.99	0.15	<i>PCK2</i>	21.16	122.11	0.17
<i>IGF1R</i>	15.64	135.23	0.12	<i>PIK3C2B</i>	15.88	104.02	0.15	<i>DMPK</i>	21.92	126.32	0.17
<i>ITPKA</i>	14.85	127.79	0.12	<i>CSNK2B</i>	20.37	133.15	0.15	<i>FLJ40852</i>	18.29	104.46	0.18
<i>GRK5</i>	16.96	143.97	0.12	<i>ULK3</i>	16.53	106.65	0.15	<i>HK1</i>	14.70	83.05	0.18
<i>ULK4</i>	12.27	101.64	0.12	<i>PHKA1</i>	19.94	126.97	0.16	<i>PIK3CA</i>	24.14	136.33	0.18
<i>PDGFRb</i>	13.84	113.67	0.12	<i>ITPKB</i>	21.40	133.28	0.16	<i>NME3</i>	17.93	101.08	0.18
<i>GCK</i>	17.09	137.69	0.12	<i>PRKCB</i>	19.27	119.87	0.16	<i>ROR1</i>	22.09	124.51	0.18
<i>PIK3CB</i>	16.14	125.79	0.13	<i>IKKB</i>	22.50	139.32	0.16	<i>PIM1</i>	22.26	124.91	0.18
<i>POLR2K</i>	12.89	100.40	0.13	<i>FGFR2</i>	19.70	121.47	0.16	<i>GUCY2F</i>	26.07	145.01	0.18
<i>TTBK1</i>	10.49	80.87	0.13	<i>PAK2</i>	18.92	116.60	0.16	<i>MYLK</i>	23.13	127.65	0.18
<i>DDR1</i>	12.04	92.32	0.13	<i>CSNK1G2</i>	16.51	101.72	0.16	<i>DYRK1B</i>	18.63	102.76	0.18
<i>JAK3</i>	14.69	111.88	0.13	<i>DGKA</i>	24.02	147.79	0.16	<i>CSNK1D</i>	25.25	138.84	0.18
<i>PHKG1</i>	17.24	130.63	0.13	<i>RAPGEF3</i>	18.40	112.44	0.16	<i>DGKG</i>	24.27	133.14	0.18
<i>PI4KB</i>	13.43	100.29	0.13	<i>PCK1</i>	18.32	110.71	0.17	<i>PRKDC</i>	22.94	125.04	0.18
<i>CSNK1E</i>	15.27	111.62	0.14	<i>PDPK1</i>	21.03	126.80	0.17	<i>PIK3C2G</i>	22.24	120.85	0.18

Table 2. 2nd screening using the siRNA library for kinases in KTC3 cells.

Gene	sphere formation (%)	cell survival (%)	sphere/survival ratio	Gene	sphere formation (%)	cell survival (%)	sphere/survival ratio	Gene	sphere formation (%)	cell survival (%)	sphere/survival ratio
<i>IKBKB</i>	2.30	100.57	0.02	<i>PIK3CB</i>	28.63	111.23	0.26	<i>NME1-NME2</i>	36.75	105.40	0.35
<i>ULK4</i>	2.56	100.87	0.03	<i>PIK3C2B</i>	25.85	100.30	0.26	<i>PHKA1</i>	38.03	108.79	0.35
<i>ULK4</i>	6.62	101.50	0.07	<i>MAPK1</i>	29.70	114.96	0.26	<i>LIMK2</i>	39.98	106.17	0.38
<i>IRAK2</i>	9.52	118.09	0.08	<i>PDK4</i>	28.42	108.69	0.26	<i>PIK3C2G</i>	41.24	106.38	0.39
<i>LOC442075</i>	8.12	98.68	0.08	<i>PHKG2</i>	26.71	100.25	0.27	<i>PRKCQ</i>	39.10	100.32	0.39
<i>PLK3</i>	11.49	104.71	0.11	<i>MAPKAPK3</i>	29.91	110.60	0.27	<i>NRK</i>	42.09	107.94	0.39
<i>PHKG1</i>	14.74	108.74	0.14	<i>MAPK9</i>	28.21	103.37	0.27	<i>CDC42BPG</i>	40.60	101.28	0.40
<i>PRKG1</i>	16.03	107.21	0.15	<i>PIM1</i>	30.77	108.04	0.28	<i>MYLK</i>	42.86	106.38	0.40
<i>TTBK1</i>	15.81	98.90	0.16	<i>PLK5P</i>	27.35	95.50	0.29	<i>PIK3CA</i>	42.52	105.05	0.40
<i>MAP2K1</i>	17.52	103.84	0.17	<i>PFKM</i>	31.62	109.55	0.29	<i>PCTK1</i>	43.31	106.68	0.41
<i>PRKDC</i>	19.23	111.79	0.17	<i>TIE1</i>	31.41	108.51	0.29	<i>PFKFB2</i>	44.02	105.23	0.42
<i>MPP3</i>	19.05	106.85	0.18	<i>DYRK1B</i>	29.27	99.79	0.29	<i>PCK1</i>	46.26	110.40	0.42
<i>GAK</i>	19.05	99.49	0.19	<i>CSNK1G2</i>	29.19	98.05	0.30	<i>CSK</i>	47.99	114.38	0.42
<i>AURKA</i>	21.79	101.33	0.22	<i>MAPK7</i>	33.33	110.12	0.30	<i>PRKCB</i>	45.09	106.97	0.42
<i>NPR2</i>	23.81	110.65	0.22	<i>MST1R</i>	32.84	105.52	0.31	<i>PLK5P</i>	43.80	101.99	0.43
<i>IGF1R</i>	23.56	109.14	0.22	<i>FGFR4</i>	31.57	99.63	0.32	<i>GUCY2F</i>	44.05	101.55	0.43
<i>ULK3</i>	23.08	104.76	0.22	<i>PRKAB1</i>	35.26	109.93	0.32	<i>POLR2K</i>	47.65	108.83	0.44
<i>PAK1</i>	23.81	107.83	0.22	<i>RAPGEF3</i>	36.54	109.46	0.33	<i>CSNK1D</i>	43.64	99.55	0.44
<i>PIM3</i>	21.58	93.31	0.23	<i>PDPK1</i>	35.47	105.80	0.34	<i>PANK3</i>	47.65	106.40	0.45
<i>TJP1</i>	23.50	101.62	0.23	<i>RIOK1</i>	34.62	102.68	0.34	<i>STK32B</i>	49.36	106.89	0.46
<i>ITPKA</i>	23.81	102.22	0.23	<i>C9orf96</i>	33.33	98.57	0.34	<i>PDGFR b</i>	50.85	108.72	0.47
<i>EIF2AK4</i>	24.36	104.02	0.23	<i>JAK3</i>	36.08	105.35	0.34	<i>AK2</i>	50.70	106.61	0.48
<i>PLK1</i>	24.57	100.52	0.24	<i>PRKCZ</i>	36.97	106.53	0.35	<i>FLJ40852</i>	47.65	100.00	0.48

Figure legends

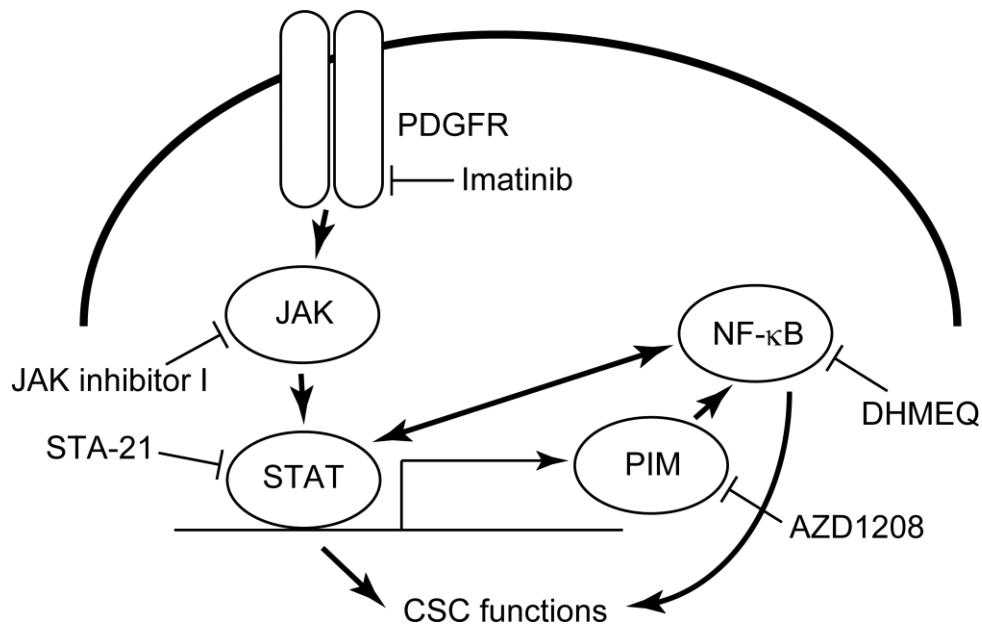
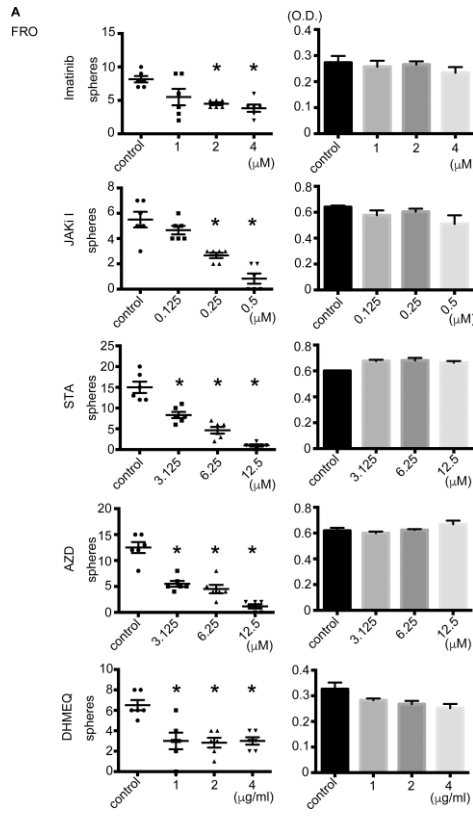


FIG. 1. The cell signaling cascade focused on in the present study. Note the crosstalks between the STAT3 and NF- κ B signaling pathways. The inhibitors used in the present study are also shown.

Thyroid

The JAK/STAT3 and NF- κ B signaling pathways regulate cancer stem cell properties in anaplastic thyroid cancer cells. (DOI: 10.1089/thy.2018.0212)
This paper has been peer-reviewed and accepted for publication, but has yet to undergo copyediting and proof correction. The final published version may differ from this proof.



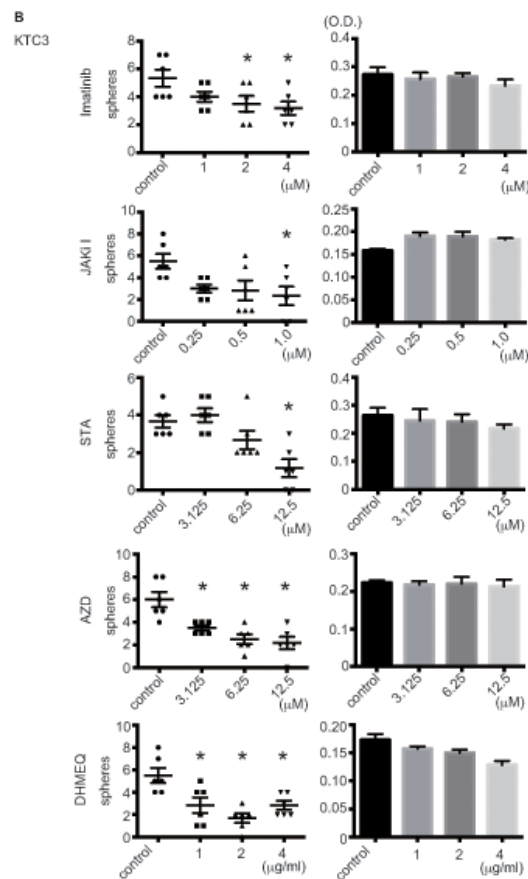


FIG. 2. The various inhibitors suppressed sphere formation but not regular cell growth in thyroid cancer cell lines. (A) (Left) Five hundred FRO cells were seeded in each well of a 96-well HydroCell plate and incubated with the indicated concentrations of the indicated inhibitors for one week. The number of spheres with a diameter $\geq 100 \mu\text{m}$ was counted and plotted. Bars represent the mean \pm SE of six wells. $*p < 0.05$ vs. control. (Right) One thousand FRO cells were seeded in each well of a regular 96-well plate. On the next day, the GM was replaced with the medium containing the indicated concentrations of the selected inhibitors. After three days of culture, cell survival was measured using a Cell Counting Kit-8. The data are shown as the mean \pm SE of three wells. Similar results were obtained in at least two independent experiments. O.D., optical density. (B) (Left) Three hundred KTC3 cells were seeded in each well of a 96-well HydroCell plate and incubated with the indicated concentrations of the selected inhibitors for one week. The number of spheres with a diameter $\geq 100 \mu\text{m}$ was counted and plotted. Bars represent the mean \pm SE of six wells. $*p < 0.05$ vs. control. (Right) One thousand KTC3 cells were seeded in each well of a regular 96-well plate. On the next day, the GM was replaced with the medium

containing the indicated concentrations of the selected inhibitors. After three days of culture, cell survival was measured using a Cell Counting Kit-8. Data are shown as the mean \pm SE of three wells. Similar results were obtained in at least two independent experiments. O.D., optical density.

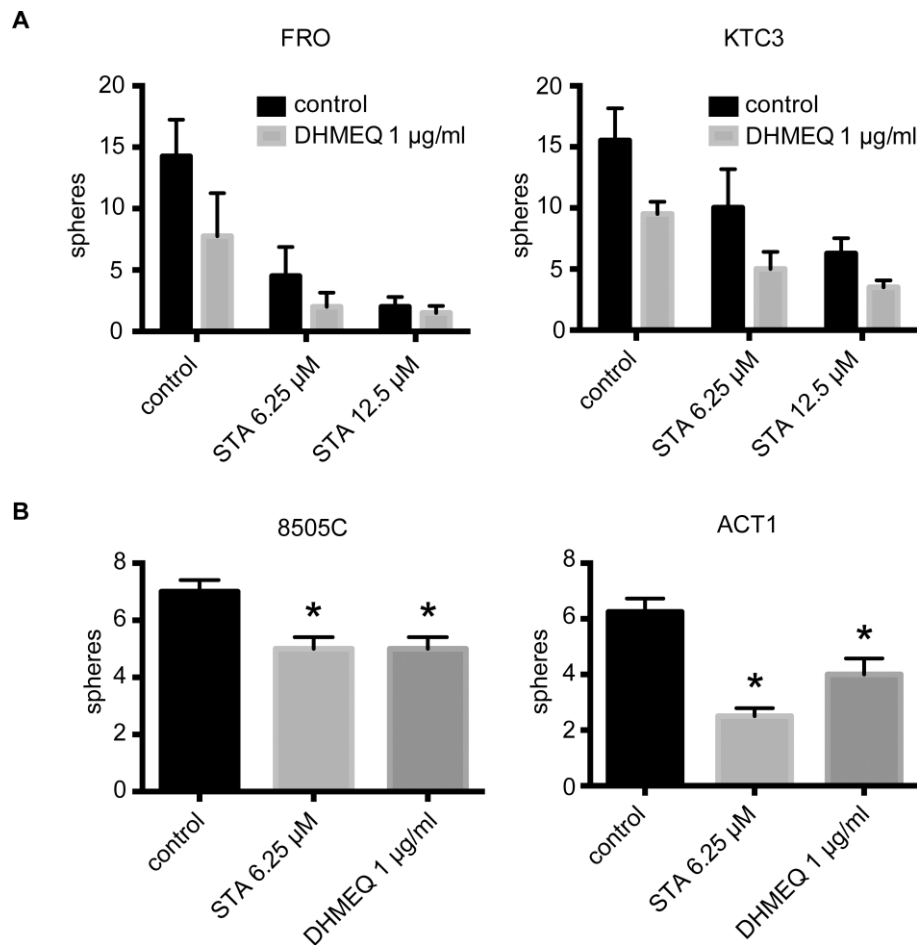


FIG. 3. (A) The effect of the combination of inhibitors for the STAT3 and NF- κ B pathways on sphere formation. One thousand FRO cells (left) or KTC3 cells (right) were seeded in each well of a 96-well HydroCell plate and incubated with the indicated concentrations of the selected inhibitors for one week. The number of spheres with a diameter $\geq 100 \mu\text{m}$ was counted. Bars represent the mean \pm SE of four wells. (B) Inhibitors for the STAT3 and NF- κ B pathways also suppressed sphere formation in 8505C and ATC1 cells. One thousand 8505C cells (left) or ATC1 cells (right) were seeded in each well of a 96-well HydroCell plate and incubated with the indicated concentrations of the selected inhibitors for one week. The number of spheres with a diameter $\geq 100 \mu\text{m}$ was counted. Bars represent the mean \pm SE of four wells. * $p < 0.05$ vs. control. Similar results were obtained in at least two independent experiments.

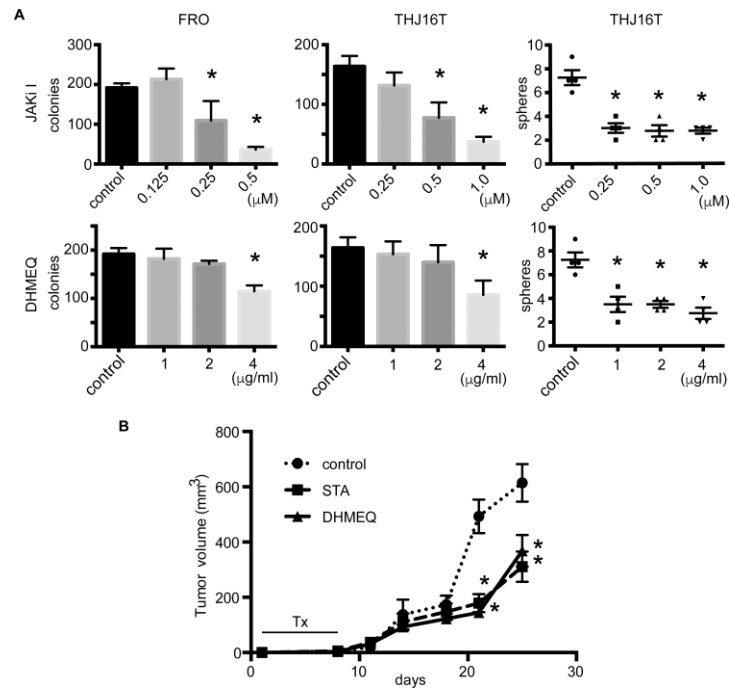


FIG. 4. (A) (Left and middle) The JAK and NF- κ B inhibitors suppressed anchorage-independent growth in soft agar. One thousand FRO cells or two thousand THJ16T cells were plated in soft agar in each well of a 12-well plate and incubated for 10 (FRO) or 20 (THJ16T) days with the indicated concentration of the selected inhibitors. The number of colonies is shown as the mean \pm SD of three wells. * $p < 0.05$ vs. control. Similar results were obtained in at least two independent experiments. (Right) One thousand and five hundred THJ16T cells were seeded in each well of a 96-well HydroCell plate and incubated with the indicated concentrations of the selected inhibitors for one week. The number of spheres with a diameter $\geq 100 \mu\text{m}$ was counted and plotted. Bars represent the mean \pm SE of six wells. * $p < 0.05$ vs. control. (B) The STAT3 and NF- κ B inhibitors suppressed tumor growth in nude mice. FRO cells (1×10^6) were implanted as described in Materials and Methods. STA-21 was injected *i.p.* at a dose of $0.5 \mu\text{g/kg/day}$ for seven days, beginning on day 1 after tumor cell implantation. DHMEQ was injected *i.p.* at a dose of $5.0 \mu\text{g/kg/day}$ on the same schedule as STA-21. Control group mice received vehicle injections only. Data are presented as the mean \pm SE of 12 tumors (in six mice). * $p < 0.05$ vs control. Tx: drug injection

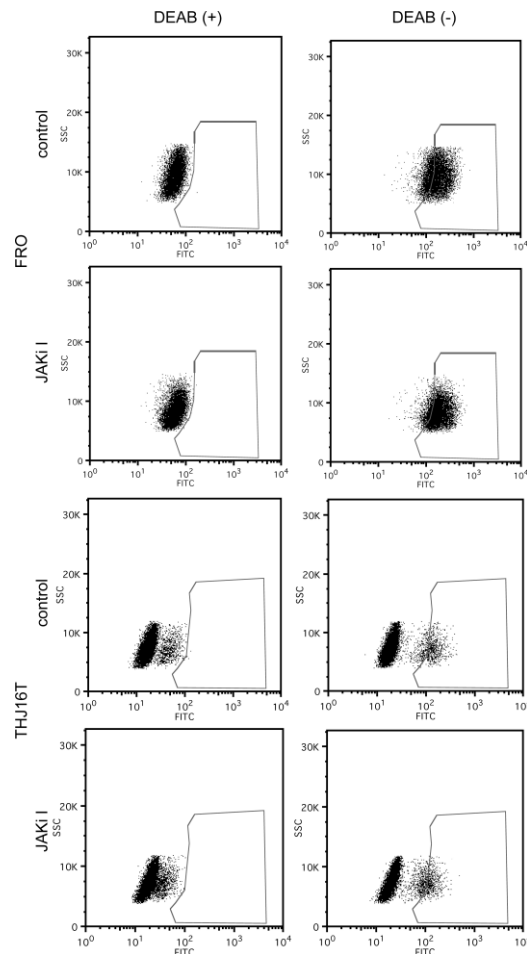
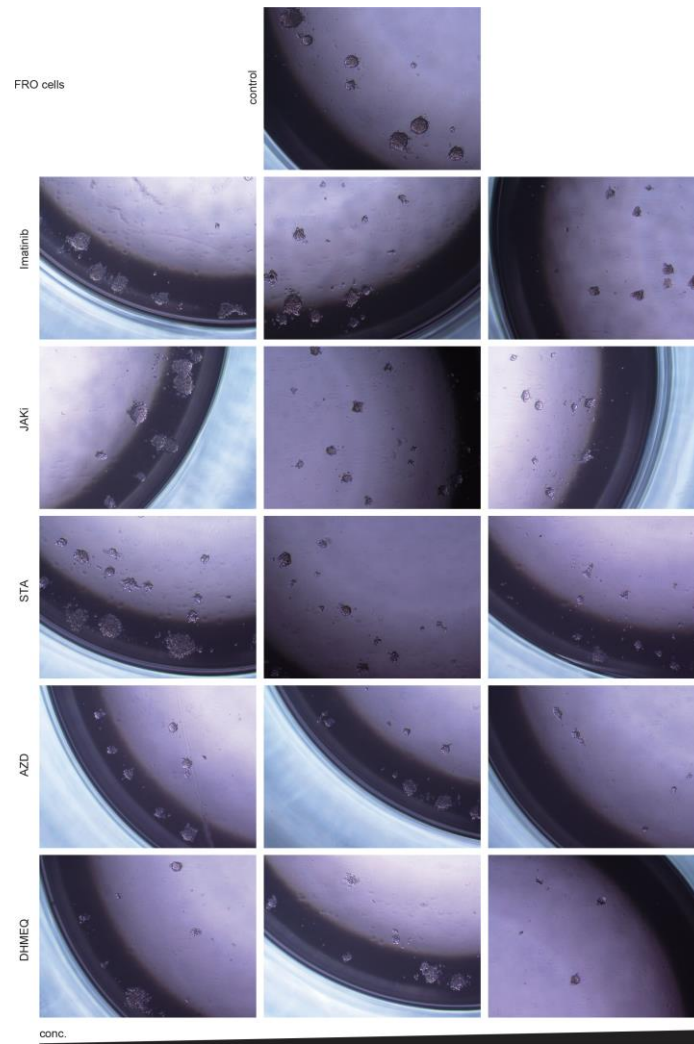


FIG. 5. The JAK inhibitor I did not alter the ALDH activity. FRO and THJ16T cells were cultured in the presence of 0.5 μ M of JAK inhibitor I for one week, and subjected to the ALDEFLUOR assay. The cells incubated in the presence of DEAB was first analyzed as a negative control (left) to set a region to distinguish ALDH negative/positive cells, and then the test samples were measured (right). Similar results were obtained in at least two independent experiments.

Thyroid

The JAK/STAT3 and NF- κ B signaling pathways regulate cancer stem cell properties in anaplastic thyroid cancer cells. (DOI: 10.1089/thy.2018.0212)
This paper has been peer-reviewed and accepted for publication, but has yet to undergo copyediting and proof correction. The final published version may differ from this proof.



Supplementary Figure legends

FIG. S1a.

Five hundred FRO cells were seeded in each well of a 96-well HydroCell plate and incubated with the concentrations (same as FIG. 2A) of the indicated inhibitors for one week. The sphere images were captured using a phase contrast microscope (40X).

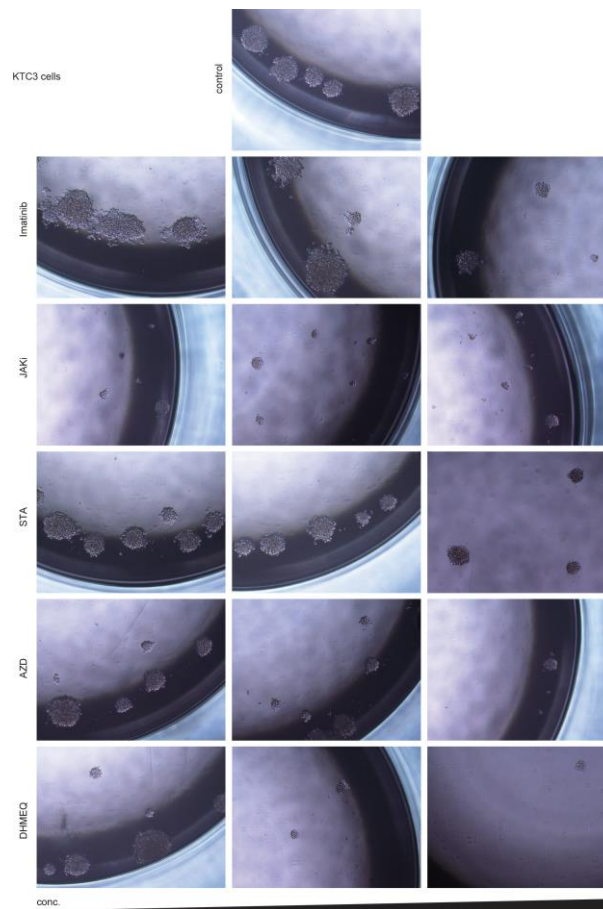


FIG. S1b.

Three hundred KTC3 cells were seeded in each well of a 96-well HydroCell plate and incubated with the concentrations (same as FIG. 2B) of the indicated inhibitors for one week. The sphere images were captured using a phase contrast microscope (40X).